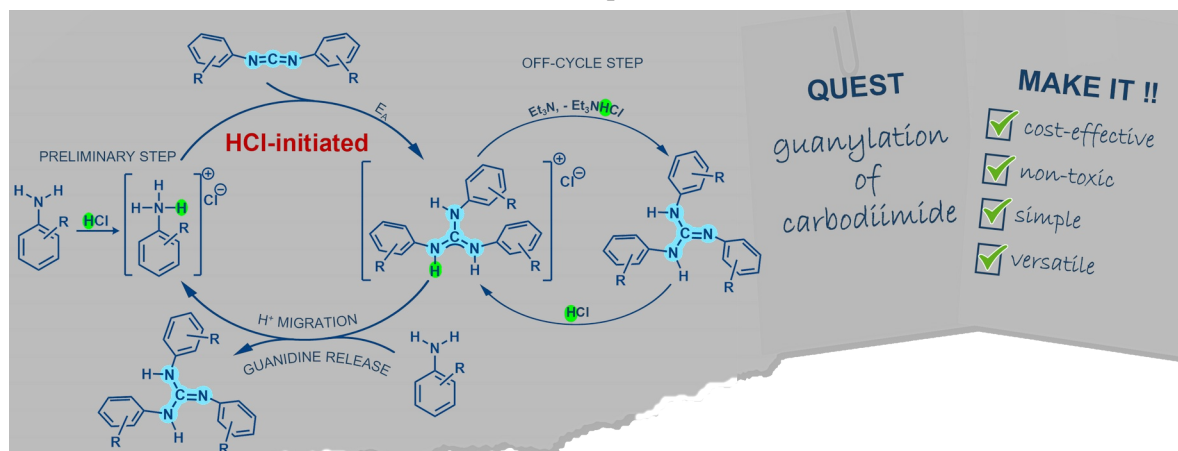


Comprehensive Reinvestigation of Carbodiimide Guanylation: HCl-initiated Access to Tri- and Tetrasubstituted Guanidines

Lukáš Vlk,^a Karel Pauk,^b Maksim A. Samsonov,^a Zdeňka Růžičková,^a Tomáš Chlupatý,^{a,*} Aleš Růžička^{a,*}

^aDepartment of General and Inorganic Chemistry, Faculty of Chemical Technology, University of Pardubice, Studentská 573, CZ-532 10, Pardubice, Czech Republic.

^bInstitute of Organic Chemistry and Technology, Faculty of Chemical Technology, University of Pardubice, Studentská 573, CZ-532 10, Pardubice, Czech Republic.



ABSTRACT: Guanidines are well known π -electron-conjugated organic bases used widely in synthesis as well as industry, with more than 150 years of history. Hence a plethora of synthetic approaches leading to the formation of the central N_3C motif has been published, from conventional methods to more sophisticated catalysts. Despite that, some substrates are still not easily obtainable and the reported procedures lack simplicity and universality. Here, procedures yielding guanidines from carbodiimides and various amines are provided. Thermally conducted reactions of aliphatic amines and carbodiimides led to guanidines, but efforts to extend this method to anilines failed even with basic or some acidic catalysts. However, when HCl was added to the reaction media at $>80^\circ\text{C}$, guanidine products were successfully prepared. Thorough mechanistic investigations revealed the complexity of the guanylation including several proton transfers, the unconventional switch of the reaction mechanism to electrophilic addition, and regeneration of the catalytically active species. The process was optimized and applicable to a series of various substrates with the use of sub-stoichiometric or even catalytic amount of HCl. Guanidine structures, guanylation mechanism and prototropic tautomerism of aryl-substituted guanidines in solution were investigated by scXRD, NMR spectroscopy and DFT calculations. Optimized, easy cheap and high-yield metal-free procedure catalyzed by HCl was described.

Introduction

Guanidines are considered organic superbases due to the n - π conjugation of the central N_3C part and a push-pull effect,^{1,2} with the imino nitrogen being the most basic moiety of the molecule². The spatial arrangement and characteristics of the N -atoms surrounding the central carbon atom of the N_3C unit provide significant configurability and tunability, influenced by steric and electronic effects. In neutral form they are useful in organic

synthesis or as (non-)nucleophilic catalysts,^{1,3-9} as Barton's bases resistant to alkylation,^{4,5,10} and have been associated with a range of biological activities, which is linked to the presence of guanidine moiety in many natural products.^{11,12} Also, guanidines have been utilized in pharmaceutical,¹³ food and petrochemical industry.¹ On the other hand, guanidinium cations show exceptional stability due to effective charge delocalization (Y -aromaticity),¹⁴ robustness of the cation and ability to form hydrogen bonds, and has been used as a building block

in the design of many organic and semi-organic materials.¹⁵ Neutral and anionic forms have been widely used as ligands for the stabilization of various metals/elements in different oxidation states.¹⁶⁻²⁰

Two general routes exist for guanidine synthesis. Classical methods using nucleophilicity/basicity of amines, employ guanylation agents such as thioureas, isothioureas, aminoiminomethanesulfonic acids, cyanamides and carbodiimides, and often require activated substrates,^{21,22} increased temperature, toxic or difficult-to-achieve catalysts non-tolerant to functional groups, and/or offer low yields (Figure 1).^{16,21-24} Thiophilic metal salts like Hg(II), Cu(II) or Sc(III) acetates or chlorides are the most common.^{25,26} In the case of carbodiimides, the guanylation of aliphatic amines is feasible when only thermally conducted, but this guanylation protocol with aromatic amines is insufficient unless initiated or activated (Figure 1) by usually stoichiometric amount of an obscure/toxic initiator.

In contrast, the modern route using catalyzed carbodiimide-amine system offers accessibility of plenty of substituted carbodiimides and overcomes the classical methods' obstacles (Figure 1 – highlighted box). These methodologies can sometimes bring challenges in terms of price, air instability, availability of the catalysts together with the respect of environmental aspects. To illustrate, guanylation of aniline with CDI^{IPr} under mild conditions with low loading of half-sandwich complexes of Y, Lu, Er (and others) as catalysts achieved high to almost quantitative conversion.²⁷ The reaction of similar substrates catalyzed by the less active dinuclear Ti(IV) amido complex required longer heating.²⁸ If a high-spin NHC-containing Fe(II) imido complex is used at 5 mol % for the guanylation of aliphatic carbodiimides with a series of anilines, conversions surpass 80% at room temperature after 15 hours.²⁹ Some metal oxo-species, such as Fe(II) acetate³⁰ or ZnO nanoparticles,³¹ or Zn-S-cysteine nanoparticles³² exhibited lower efficiency. In the field of main group element complexes (Li, Mg, Al, B), similar behavior to transition metal-based catalysts was observed.³³⁻³⁷ Guanylations of diisopropylcarbodiimide with selected functionalized anilines, such as 2-bromoaniline or *p*-anisidine, initiated by tris(pentafluorophenyl)borane,³⁸ also reveal good effectiveness for activated substrates. SnCl₄ was used to catalyze annulation of 2-aminobenzonitrile and carbodiimides recently.³⁹ During the completing of this work, the guanylation of aliphatic amines, anilines, (sulfon)amides, ureas, and carbamates by guanidinium salt (HATU), leading to pentasubstituted guanidines, was described.⁴⁰

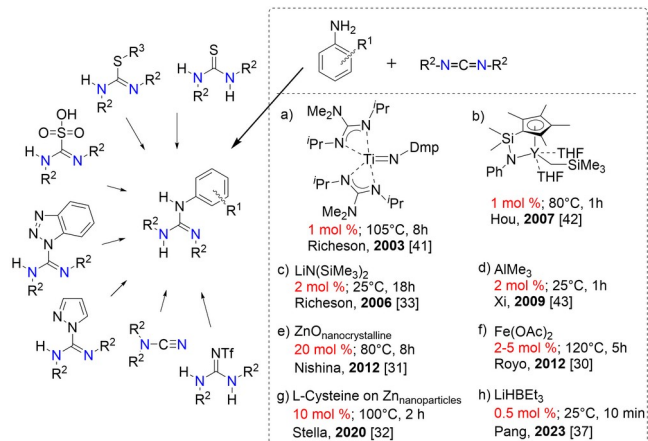


Figure 1. Overview of classical approaches for guanylation reactions of amines. Guanylation protocol of carbodiimide and aromatic amines using selected catalysts is highlighted in the box. Appropriate references are given in square brackets.

As illustrated in Figure 1, there is a plethora of excellent catalytic systems for the guanylation of carbodiimide described in the literature able to achieve high conversion at mild conditions or using relatively cheap commercially available chemicals (for example Me₃Al). However, none of these systems reaches all characteristics of an all-round/universal catalyst, and the protocols suffer from drawbacks such as the use of a (sometimes toxic) metal or are limited by the scope. The most effective catalysts are usually unavailable and sensitive to moisture, while the air-stable species require much higher loading due to lower efficiency (ZnO nanoparticles). This work has the ambition to fulfill the requirements of a simple synthesis of structurally and electronically flexible guanidines while making the synthetic protocol cheap, green, unified, substrate universal and atom-efficient

Results and Discussion

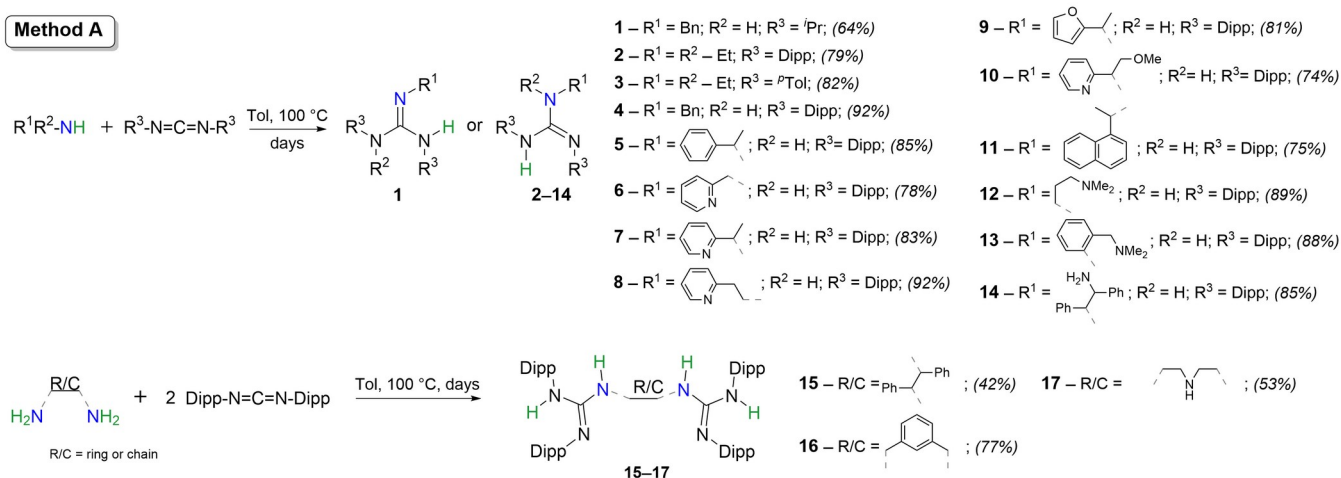
Guanidines **1–17** (Scheme 1) were prepared by a classical guanylation approach²¹ via non-catalyzed thermal nucleophilic addition of an amine to a polarized cumulated NCN double bonds of the carbodiimide moiety in commercial grade toluene at 100 °C for day(s) (dependent on the nature of the amine and monitored by ¹H NMR spectroscopy) – **Method A** (for a list of compounds see Figure S1 in ESI). Various aliphatic amines and diamines (including also (hetero)aromatic moiety) and *N,N*-disubstituted carbodiimides (Pr, ^{*n*}tol, Dipp) gave appropriate guanidines of analytical purity after recrystallization/distillation in high to excellent yield. In the case of guanidine **13**, aromatic amine was used as the starting material, which can be classified more as an aliphatic amine

in this guanylation protocol because of the activation of the NH₂ group through intramolecular hydrogen bond to NMe₂ group. This subsequently results in enhanced nucleophilicity and increased basicity. Attempts to prepare the monoguanidine analogue of **16** (1:1 ratio product) ended in an equimolar mixture of mono- and

bis(guanidine) due to a competing reaction on both amino groups.

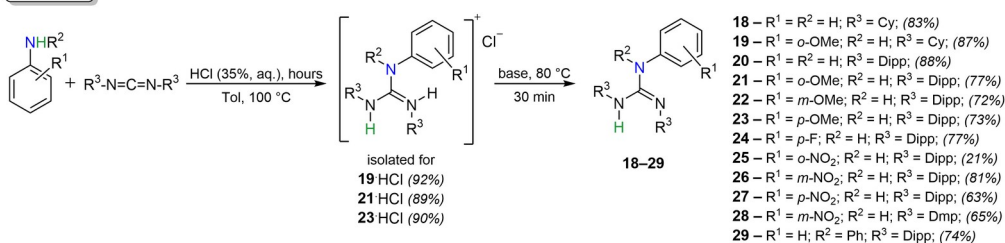
Scheme 1. Synthesis of guanidines **1-17** via non-catalyzed thermal guanylation of carbodiimides – Dipp = 2,6-diisopropylphenyl-. Isolated yields of target guanidines are given in parentheses.

Method A

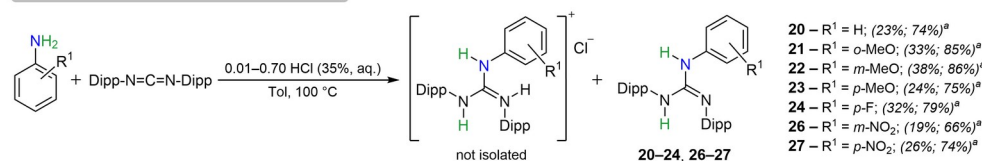


Scheme 2. Synthesis of guanidines **18-29** (and guanidiniums **19**·HCl, **21**·HCl and **23**·HCl) via the HCl-initiated guanylation of carbodiimides. Base – Et₃N (^tBuOK for **19**·HCl). Isolated yields of target guanidines (**Method B**) and NMR yields after 2 days using 50 mol % of HCl (**Method C**) are given in parentheses where the first number^a corresponds to free guanidine and second to sum of free guanidine and its guanidinium.

Method B



Method C - substoichiometric amount of HCl



To broaden the scope to anilines, the protocol effective for aliphatic amines failed. No guanidine products were detected by NMR spectroscopy even after prolonged heating of the mixture of CDIs and anilines. Similarly, acid or base catalysis (NaOH or CH₃COOH) or the introduction of donor functional groups to the aniline did not yield successful results. Surprisingly, the addition of a

few drops of aqueous HCl (the same result was obtained with anhydrous HCl/CPME solution under Ar) at 100 °C in toluene caused the formation of guanidine (**21**) along with the corresponding guanidinium. No conversion was detected by NMR spectroscopy below 80 °C. The reaction mixture was further treated with a base (Et₃N or ^tBuOK), and only guanidine was obtained, which in-

spired further investigation for various substrates using a defined amount of HCl.

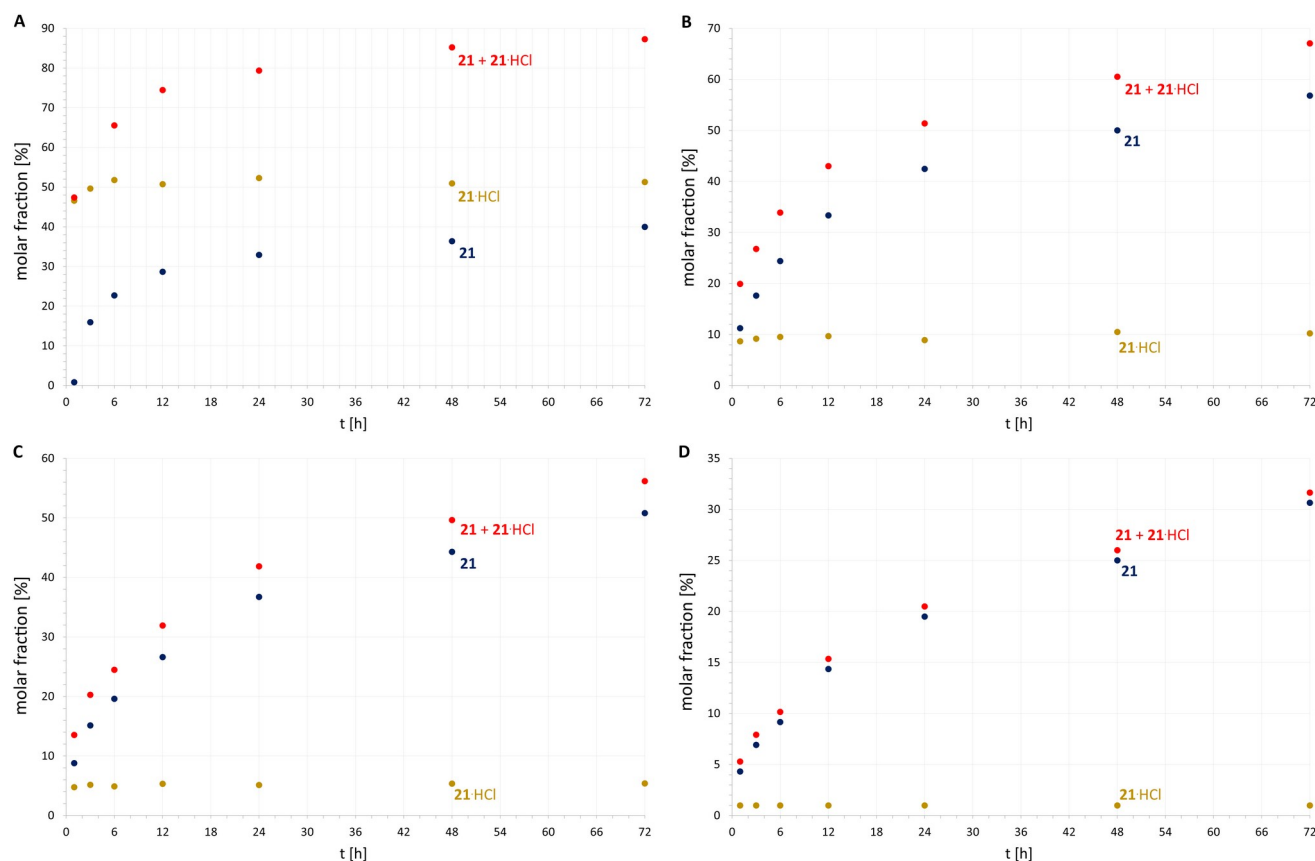


Figure 2. NMR yields of guanylation reactions of CDI^{Dipp} by *o*-anisidine to **21** (blue dots), **21·HCl** (gold dots) or to cumulative yield of **21** and **21·HCl** (red dots) using **A**) 50 mol % of HCl; **B**) 10 mol % of HCl; **C**) 5 mol % of HCl and **D**) 1 mol % of HCl after 3 days.

First trials conducted for reactions of *o*- or *p*-anisidine with CDI^{Dipp} and a stoichiometric amount of HCl (Scheme 2 - **Method B**) yielded the conjugated acids of **21** and **23** (denoted as **21·HCl** and **23·HCl**) quantitatively after 1 hour. However, these reactions ended at the guanidinium form, which requires an additional neutralization step and thus may, in some cases, be complex. This approach was extended to other primary aromatic amines (*o*-/*m*-/*p*-MeO, *p*-F, *o*-/*m*-/*p*-NO₂) and substituted CDIs (Cy, Dipp, Dmp), resulting in guanidines **18-28** (Scheme 2 and Figure S2 in ESI) after 12 hours of heating in toluene, followed by *in situ* neutralization by Et₃N (or *t*-BuOK in THF for isolated **19·HCl**). During the review process of this paper, the most challenging system was identified by one of the reviewers. As a proof-of-concept evaluation one tetrasubstituted tertaarylguanidine **29** was successfully prepared under identical protocol. To prevent the easy oxidation of the aliphatic CDI under acidic conditions, the guanylations to **18** and **19** were performed under an inert argon atmosphere. Unexpectedly, during the synthesis of **25**, which originated from an aromatic CDI and *o*-nitroaniline, a significant amount of urea (as well as its protonated form) was observed,

even when the reaction was conducted under argon. A negligible increase of **25** yield (21% to 28%) was achieved when the amount of HCl was reduced to 50 mol %.

During the guanylation of the aniline series, it became evident that HCl plays a pivotal role in the reaction mechanism, indicating greater complexity of the process. To elucidate this mechanism further, the impact of varying sub-stoichiometric/catalytic amounts of HCl on the guanylation of aromatic substrates was investigated (Scheme 2 - **Method C**). Specifically, the synthesis of **21** (also hidden in **21·HCl**) from *o*-anisidine and CDI^{Dipp} was examined using 1–70 mol % of HCl over time (Figures 2 and S9 in ESI). The yields were quantified as a sum of guanidine (**21**) and its guanidinium (**21·HCl**), or only **21** over the duration of the reaction while the amount of guanidinium remains constant throughout the whole process and equal to the amount of HCl used (Figure 2). It should be considered that prolonged heating can lead to oxidation/degradation of substrates. The findings from the guanylation protocol suggest that using a larger amount of HCl leads to almost complete reaction (**21·HCl** predominates in the mixtures) within three days. More-

over, when a small initiator concentration (under 10 mol %) is used, there is still a significant increase in the yield of **21**, due to lower concentration of **21**·HCl. For instance, the reaction with 50 mol % of HCl produced 29% of **21** after one day, with the yield rising to only 40% by day seven. In contrast, when only 1 mol % of HCl was utilized, the yield increased from 19% to 44%. To complete this hypothesis, the catalytic efficiency was screened using 1–100% mol of HCl loading, plotted as yield against catalyst concentration (Figure 3), showing maximum yield to **21** at 25 mol % of HCl.

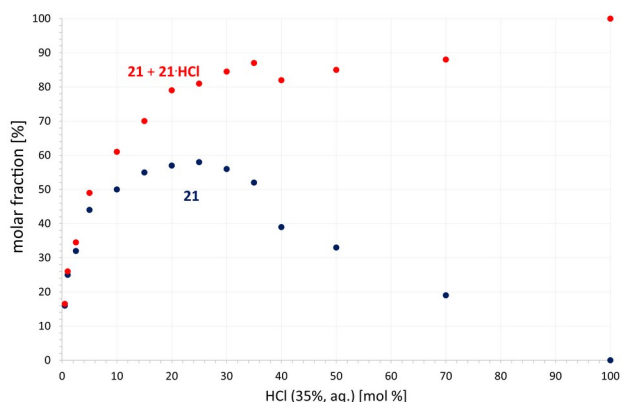


Figure 3. Optimization of the HCl amount for preparation of **21** (blue dots) or sum of **21** and **21**·HCl (red dots) after 2 days.

Expanding the portfolio of that method was applied to other anilines with addition of 10 and 50 mol % of HCl (Scheme 2 – **Method C**), covering various functional groups in different aromatic ring positions, including aniline (**20** – Figure S8), anisidines (**22–23** – Figures S10–S11), *p*-fluoroaniline (**24** – Figure S11), and nitroanilines (**26–27** – Figures S12–S13).

The overall basicity of respective aniline is a contribution of mesomeric and induction effects is the determining factor, on which the reaction course depends. For the catalytic guanylation, the essential prerequisite is anilines' high proton affinity to form a conjugated pair with HCl (anilinium). This is evident in the case of the two *meta*-substituted anilines (better-performing *m*-OCH₃ going to **22** vs. *m*-NO₂ going to **26**), also compared to unsubstituted aniline for the formation of **20** (see SI, table S2). Another comparison can be drawn between *o*-OCH₃ (**21**) and *m*-OCH₃ (**22**), where the yields to **21** are *ca* 20% higher. This was more pronounced for comparative experiments with 10% of HCl, where yields were 15% for **26**, 31% for **22**, and 42% for **21** after one day (Table S2).

All isolated guanidines **1–29**, covering all four typological combinations of starting aliphatic(R^{Alif})/aromatic(R^{Ar}) (Figure 4) amines and carbodiimides, and guanidiniums **19**HCl, **21**HCl and **23**HCl were completely characterized by multinuclear NMR, MALDI-MS, scXRD (except of **3**, **9**, **11** and **16**; Figures S16–S43 in ESI) techniques and ele-

mental analysis (**20–29**, **21**HCl and **23**HCl) (for an overview of the structural characterization methods used – see Figures S1–S2 in ESI). The most significant phenomena used for monitoring course of the reaction were the hydrogen shift(s) from the starting amino group to nitrogen atom(s) originated from the CDI moiety (change of ¹H NMR spectral pattern or chemical shift) and the related downfield shift of the central carbon atom (Ar_q^{Gua}) in ¹³C NMR spectra. In nearly solvent-independent ¹H NMR spectra, the NH hydrogen atoms are chemically non-equivalent (except for **1**, **18**, and **19**). For **13** and **25**, one NH (originating from aniline) is downfield-shifted because of an intramolecular H-bond. The deshielding of Ar_q^{Gua} was observed in ¹³C spectra for all prepared guanidines, with typical values of ~150 ppm for tri-/tetrasubstituted di-/trialkylguanidines **1–3**, **18**, **19** and **29** (measured at 240 K in Tol-d₈), while for trisubstituted di-/triarylguanidines **4–17** and **20–28**, the values range between 144–147 ppm. To complete the structural description, the C–N distances of the N₃C unit show partial π-electron delocalization for all guanidines (C^{Gua}–NH 1.36–1.39 Å and C^{Gua}–N ~1.30 Å) (Figure 4), with slight differences for tetraarylguanidine **29** (Fig. S43 caption).

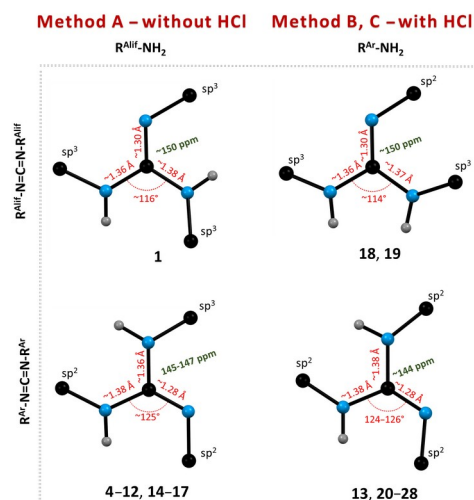


Figure 4. Illustration of selected structural parameters of guanidines, encompassing all four typological combinations. Blue spheres represent N-atoms, black for C-atoms, and gray for H-atoms. The ¹³C NMR chemical shifts of Ar_q^{Gua} are in green.

In the NMR spectra of ‘aromatic’ guanidines **20–27** and **29**, originated from the anilines and aromatic CDI^{Dipp}, a second minor set of signals with similar chemical shift values was observed. This phenomenon was more pronounced in THF-d₈ (for **29** observed in Tol-d₈ at 240 and 273 K – Figures S70–S71) solution and further investigated for an extreme example of **26** by VT-NMR spectroscopy (Figures S4–S7 in ESI) and DFT calculations (Figures 6). 18 mol % of minor form was detected at room temperature in THF-d₈, contrary to 9 mol % in C₆D₆, while only negligible temperature dependency was ob-

served by VT-NMR measurements in both solvents (see Figure S5–S7). However, significant change of relative populations of both species was observed in Tol- d_8 in the range of 183–373 K (Figure 5 and S7 in ESI).

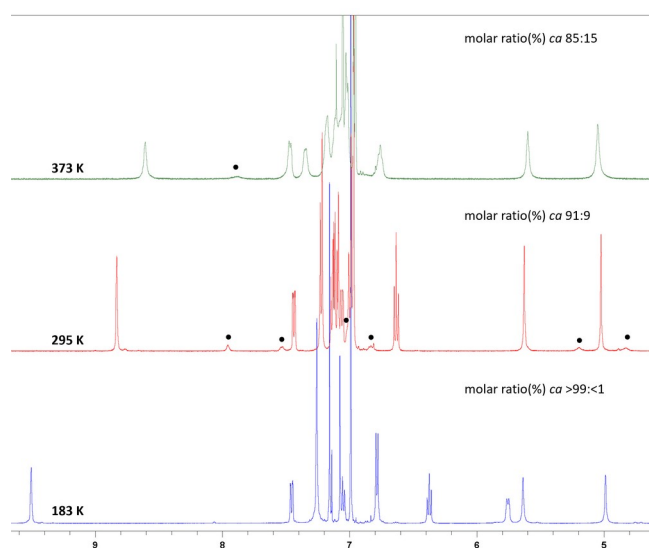


Figure 5. Detail of VT ^1H NMR spectra of **26** in Tol- d_8 at 183–373 K. Signals of the minor tautomer are marked with black dots.

This was initially attributed to a prototropic guanidine tautomerism/isomerism. The structures of four reliable conformers/isomers constructed both from ab initio or sXRD/optimized geometries were prepared. For these species, the NMR shielding constants for ^{13}C nuclei were calculated by GIAO method (B3LYP/6-311+g(d,p)/D3/CPCM(THF)).⁴⁴ The most probable isomers/conformers of **26** were selected on the direct comparison of the structures, Gibbs' free energies (Figure 6)^{45,46} and calculated (Table S1, Figure S3) vs. measured ^{13}C NMR parameters in THF- d_8 solution.

Two of the four relevant isomers - specifically, the pair of rotamers **26A** and **26A'** (Figure 6)- exhibit a minimal energy difference of just 1 kcal.mol $^{-1}$ in THF (virtually identical in C_6H_6). Moreover, the rotation barrier from **26A** to **26A'** is only 3.7 kcal.mol $^{-1}$. These isomers are thus indistinguishable in solution by NMR spectroscopy and their weighted chemical shifts represent the signals of the major isomer of **26**. According to the Boltzmann distribution at room temperature, their respective contributions to the chemical shift values are 15.4% for **26A** and 84.6% for **26A'** (Table S1, Figure S3). For isomer **26B**, analysis of the correlation between the measured signals in the ^{13}C NMR spectra and the calculated chemical shieldings indicates that it exists as a minor form in solution NMR (Table S1, Figure S3). In contrast, isomer **26C**, despite being energetically similar, was not detected in either the solution or solid state.

To provide a deeper understanding of the guanylation mechanism, we conducted a detailed investigation of the *o*-anisidine- CDI^{Dipp} -HCl system using NMR and DFT techniques at the B3LYP/cc-pVTZ level of theory.^{45,46} It clearly showed that the process began with the immediate protonation of the aniline to **INT-1** (Figure 7; rather than a less basic CDI^{Dipp}). This was also evidenced by the fast proton transfer from individually prepared $\text{H}^+\text{CDI}^{\text{Dipp}}$ and *o*-anisidine.

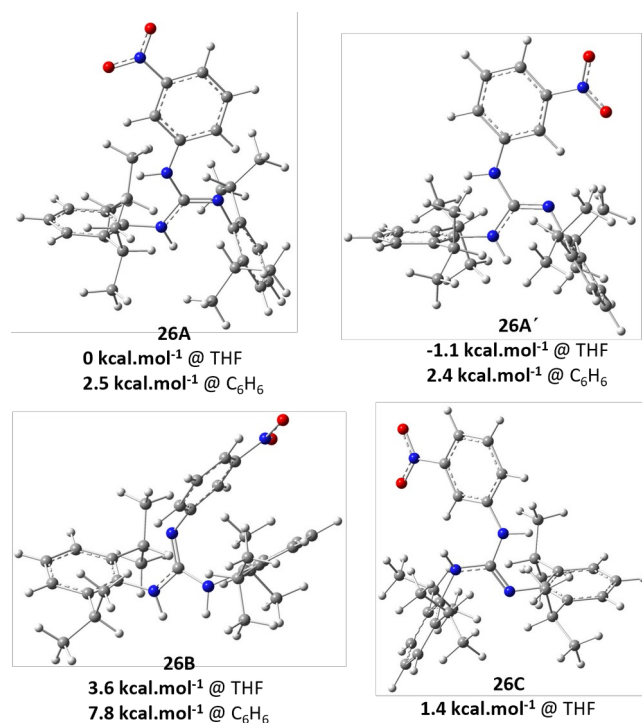


Figure 6. Optimized structures of possible tautomers/isomers of **26** along with relative Gibbs' free energies.

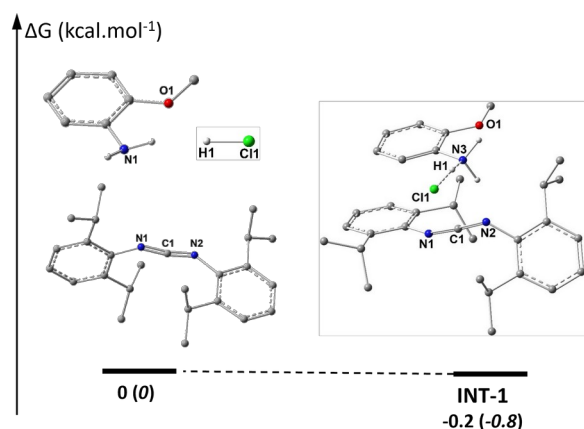


Figure 7. The DFT-estimated Gibbs free energy profile (kcal.mol $^{-1}$) for the calculated interaction between *o*-anisidine (values for *p*-anisidine are given in parentheses), CDI^{Dipp} and HCl molecule.

The thermodynamically lowest **21**·HCl species (-20.31 kcal.mol⁻¹) is produced through several consecutive steps (Figure 8 and Figure S14 in ESI), virtually connected by several H-bond interactions. From **INT-1**, the H1 from the amino group connects the aniline to the CDI of **INT-2**, bringing thus the N3 and C1 atoms into proximity. The energetically limiting step is **TS-2** (7.75 kcal.mol⁻¹), where the N3-C1 bond is formed, followed by an intramolecular proton transfer of H2 (via **INT-1** to **TS-3**). The proposed slow migration of the proton from **21**·HCl to the next starting *o*-anisidine molecule (**TS-4**, $\Delta\Delta G$ 18.67 kcal.mol⁻¹) allows the initiation of a new catalytic cycle (blue lines in profile). The guanidine **21** is released and accumulates

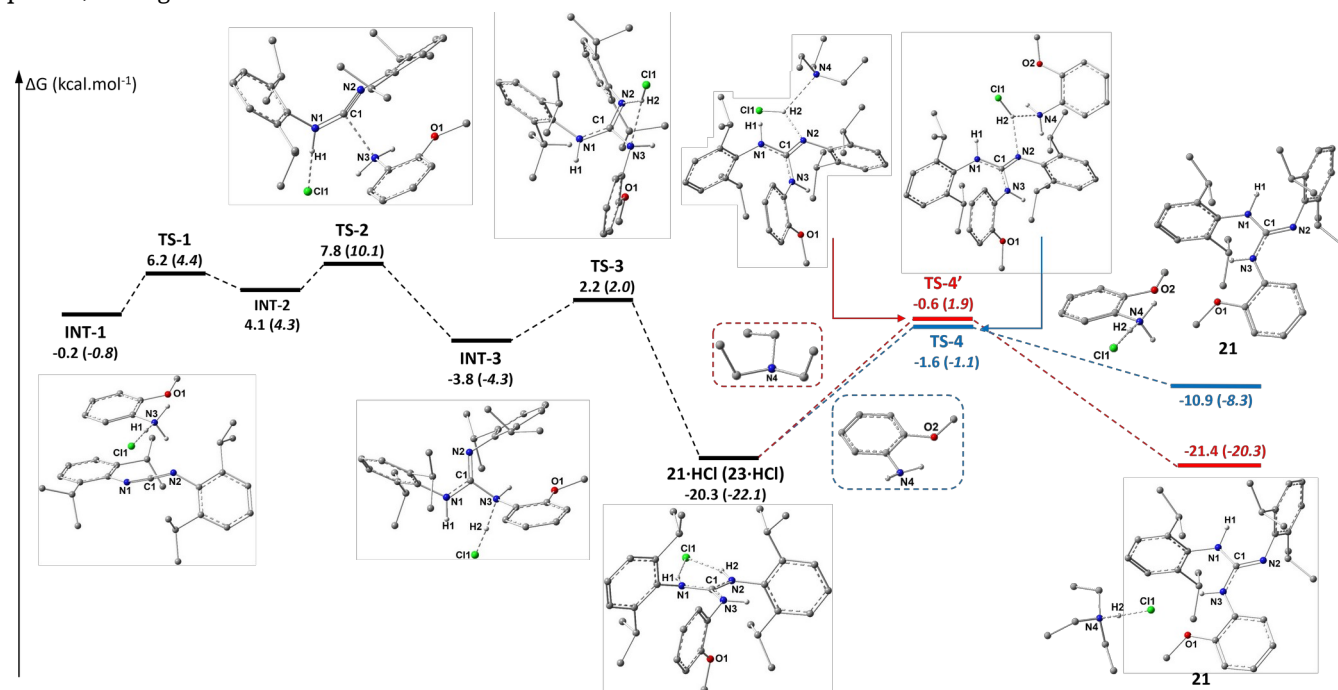


Figure 8. The DFT-estimated Gibbs free energy profile (kcal.mol⁻¹) for **21** (**23** in italics in parentheses). Preliminary step to **INT-1** (see Figure 7 - above), and structures describing **TS-1** and **INT-2** are omitted for clarity. Full energy profile is available in Figure S14 in ESI.

covering combinations of CDI-amine (aliphatic or aromatic, Figure S15), showed thermodynamically favorable catalytic processes in the series of aliphatic amines. Based on these findings, additional guanylation experiments, mimicking a sub-stoichiometric amount of acid catalyst, were successfully initiated by 50 mol % of *o*-anisidinium hydrochloride or guanidinium **21**·HCl (Scheme S1 in ESI). To be honest, there are decades-old papers reporting a few examples of ammonium salts and their interactions with carbodiimide (amine and carbodiimide in an acidic environment), but the results were misunderstood, and useful details overlooked.⁴⁷⁻⁵⁴ Taking these reports into account, a stoichiometric reaction of *o*-anisidinium and **21** in toluene was performed, yielding exclusively **21**·HCl and *o*-anisidine after 1 hour, even at room temperature (Scheme S1 in ESI).

over time, which is compensated by the fast generation of another new **21**·HCl. An alternative pathway, which is more thermodynamically favored, is the neutralization of **21**·HCl by Et₃N addition – **TS-4'** – the red trace in Figure 4. To explore the influence of a sterically less demanding substrate of the same basicity, the same calculations were performed for *p*-anisidine to provide **23** (Figure 8 in brackets), with negligible energy changes. When virtually replacing the proton, within the mechanism, for a metal ion, each individual reaction step would be similar. As expected, calculations of all four model systems,

Conclusions

There is no comprehensive guanylation approach covering a wide array of substrates respecting functional groups with low economic and accessibility requirements. It is reasonable to assert that the literature describes numerous catalytic carbodiimide guanylation systems that exhibit enhanced conversion values and reduced reaction times, however, these systems are often constrained by limitations related to the steric accessibility or reactivity of substrates, as well as the use of toxic, sensitive, or difficult-to-obtain catalysts. In contrast, this study presents a cost-effective, non-toxic, and universally applicable alternative for the synthesis of tri- and tetrasubstituted guanidines, employing HCl as an initiator. Concretely, the suggested guanylation mechanism (to **21**) was supported by extended model experiments and theoretical calculations. The rate determining

step, connected to the highest computed activation barrier for **TS-4** (release of **21**, $\Delta\Delta G$ 18.67 kcal.mol⁻¹), corresponds to the proton transfer from earlier formed guanidinium to adjacent molecule of aniline. The reaction time can be drastically shortened by employing higher amount of HCl followed by the addition of stronger base with subsequent work-up.

Materials and methods

All solvents and chemical reagents were purchased from commercial sources, and used without further purification. Some synthetic procedures were performed using the standard Schlenk techniques under an inert argon atmosphere (99.999%) (inert gas was passed through the oxygen/moisture trap Supelco before entering the vacuum/inert line) and solvents were dried with the help of solvent purification system PureSolv MD 7 supplied by Innovative Technology, Inc., degassed and then stored under argon atmosphere over a potassium or sodium mirror, if needed. Single crystals suitable for X-ray analysis were obtained from corresponding saturated solutions of products in organic solvent(s) cooled to 7 or -30 °C or by slow evaporation at room temperature. Deuterated solvents for NMR spectroscopy, if needed, were distilled, degassed, and stored over a K or Na-mirror under an argon atmosphere.

Elemental analysis (C, H, N, Cl) were performed on an automatic microanalyser Flash 2000 Organic elemental analyzer. Mass spectrometry with high resolution was determined by the “dried droplet” method using a MALDI mass spectrometer LTQ Orbitrap XL (Thermo Fisher Scientific) equipped with a nitrogen UV laser (337 nm, 60 Hz). Spectra were measured in positive ion mode and in regular mass extent with a resolution of 100,000 at a mass-to-charge ratio (m/z) of 400, with 2,5-dihydrobenzoic acid (DHB) used as the matrix. Mass spectrum of **29** was performed on Vanquish HPLC/ISQ system from Thermo Scientific equipped with quaternary pump (VC-P20-A), split sampler (VC-A12-A), column compartment (VC-C10-A), diode array detector (VC-D11-A) and mass spectrometer (ISQ ICMS Family).

NMR spectra were recorded from solutions of appropriate compounds in deuterated solvent(s) on a Bruker Avance 500 spectrometer (equipped with a Z-gradient 5 mm Prodigy™ cryoprobe) at frequencies for ¹H (500.13 MHz), ¹³C{¹H} (125.76 MHz) and ¹⁵N (50.66 MHz) or a Bruker UltraShield™ 400 spectrometer at frequencies for ¹H (400.13 MHz), ¹³C{¹H} (100.58 MHz) at 295 K or in some cases at various temperatures. Solutions were obtained by dissolving approximately 40 mg of each compound approximately in 0.6 ml of deuterated solvents. Values of ¹H chemical shifts were calibrated to residual signals of benzene ($\delta(^1\text{H}) = 7.16$), THF ($\delta(^1\text{H}) = 1.73$), toluene ($\delta(^1\text{H}) = 2.09$) or DMSO ($\delta(^1\text{H}) = 2.50$). Values of ¹³C chemical shifts were calibrated to signals of THF ($\delta(^{13}\text{C}) = 67.6$), benzene

($\delta(^{13}\text{C}) = 128.4$), toluene ($\delta(^{13}\text{C}) = 20.4$) or DMSO ($\delta(^{13}\text{C}) = 20.4$) and ¹⁵N to external nitromethane ($\delta(^{15}\text{N}) = 0.0$). All ¹³C NMR spectra were measured using a standard proton-decoupled experiment and CH and CH₃ vs. C and CH₂ were differentiated with the help of the APT method.⁵⁵ Determination of signals of chemically nonequivalent protons, carbon and nitrogen atoms in the NMR spectra were supported by ¹H,¹H-COSY, ¹H,¹H-NOESY, ¹H,¹³C-HSQC or/and ¹H,¹³C-HMBC techniques.

General methods for guanylation reactions (1 – 29)

Method A: Guanylation without HCl (1 – 17)

To a round-bottom flask equipped with condenser, one equivalent of colorless *N,N*-diisopropylcarbodiimide, 1,3-di-*p*-tolylcarbodiimide or *N,N*-bis(2,6-diisopropylphenyl)carbodiimide with one (or half) equivalent of appropriate aliphatic (except **13**) amine/diamine was dissolved in toluene. The reaction mixture was refluxed for several days, depending on the type of amine (**2** – **19** days). After that, the toluene was evaporated under vacuum, and crude products were purified by recrystallization from organic solvent(s) or by distillation (for **1**).

Method B: Guanylation with stoichiometric amount of HCl (18–29, 19HCl, 21HCl and 23HCl)

To a round-bottom flask equipped with condenser, one equivalent of colorless *N,N*-dicyclohexylcarbodiimide, *N,N*-bis(2,6-dimethylphenyl)carbodiimide or *N,N*-bis(2,6-diisopropylphenyl)carbodiimide with one equivalent of appropriate aromatic amine was dissolved in toluene followed by addition of same equivalent of HCl solution. The reaction mixture became heterogeneous and was heated to 100 °C overnight with subsequent cooling to room temperature. Appropriate crude guanidinium chlorides were formed.

In the case of **19**HCl, **21**HCl and **23**HCl crude products were additionally isolated by filtration and purified by washing/recrystallization from organic solvent. However, for **25**, all solvents from the reaction mixture were evaporated, crude product (mainly guanidinium) washed by a big portion of Et₂O and suspended in hexane.

Then 1.1 equivalent of Et₃N was added into the mixture (all protonated forms were transformed to their neutral species) which led to gradual precipitation of white solid of Et₃NHCl for 30 min at 80 °C (except **19**HCl – ^tBuOK in THF). After that, prepared guanidines **19** – **28** were filtered off, toluene evaporated under vacuum, and crude products were purified by recrystallization from organic solvent(s). Detail complex purification process of **18** is described below.

Method C: Guanylation with sub-stoichiometric amount of HCl (20 – 24, 26 - 27)

To a round-bottom flask equipped with condenser, colorless *N,N*-bis(2,6-diisopropylphenyl)carbodiimide (0.5 g,

1.38 mmol) with one equivalent of appropriate aromatic amine was dissolved in toluene (30 ml) followed by addition of sub-stoichiometric amount of HCl solution (35% aqueous solution, $\rho = 1.180 \text{ g}\cdot\text{cm}^{-3}$), which caused immediate formation of white precipitate (related to amount of HCl). The reaction mixture was heated to 100 °C for a certain period, which depends on degree of conversion monitored by integration of ^1H NMR spectra in THF- d_6 of reaction mixture aliquots in timeline.

In some cases, Et_3N (10% excess relative to HCl) was added into the mixture, which led to gradual precipitation of white solid of $\text{Et}_3\text{N}\cdot\text{HCl}$ in 30 min at 80 °C. All protonated forms were transformed to their neutral species, to confirm the amount of formed guanidines, determined by NMR yield without further isolation/purification.

Crystallography

Full-set of diffraction data for **2**, **4–8**, **10**, **12–14** and **17** (see Tables S4–S13 and Table S15) were obtained at 150 K using Oxford Cryostream low-temperature device on a Nonius KappaCCD diffractometer with MoK_α radiation ($\lambda = 0.71073 \text{ \AA}$), a graphite monochromator, and the ϕ and χ scan mode. Data reductions were performed with DENZO-SMN.⁵⁶ The absorption was corrected by multi-scan method – SADABS or by integration methods.⁵⁷ Structures were solved by direct methods (Sir92)⁵⁸ and refined by full matrix least-square based on F^2 (SHELXL97).⁵⁹

Full-set of diffraction data for **1**, **15**, **18–29**, **19HCl**, **21HCl** and **23HCl** (see Table S3, Table S14 and Tables S16–S30) were collected at 150(2)K with a Bruker D8-Venture diffractometer equipped with Cu ($\text{Cu}/\text{K}_\alpha$ radiation; $\lambda = 1.54178 \text{ \AA}$) or Mo ($\text{Mo}/\text{K}_\alpha$ radiation; $\lambda = 0.71073 \text{ \AA}$) micro-focus X-ray (μS) sources, Photon CMOS detector and Oxford Cryosystems cooling device was used for data collection.

The frames were integrated with the Bruker SAINT software package using a narrow frame algorithm. Data were corrected for absorption effects using the Multi-Scan method (SADABS). Obtained data were treated by XT-version 2014/5 and SHELXL-2017/1 software implemented in APEX3 v2016.5-0 (Bruker AXS) system.⁶⁰

Hydrogen atoms were mostly localized on a difference Fourier map, however, to ensure uniformity of treatment of crystal, all hydrogen atoms were recalculated into idealized positions (riding model) and assigned temperature factors $H_{\text{iso}}(\text{H}) = 1.2 U_{\text{eq}}$ (pivot atom) or of $1.5U_{\text{eq}}$ (methyl). H atoms in methyl, methylene, moieties and hydrogen atoms in aromatic rings were placed with C–H distances of 0.96, 0.97, and 0.93Å. Hydrogen atoms of N–H groups were refined freely or with fixed distances of 0.92Å. Disordered parts of isopropyl and coordinated THF molecules in **1** were treated by standard methods.

Crystallographic data for structural analysis have been deposited with the Cambridge Crystallographic Data Centre, CCDC no. 2120564–2120577, 2120580–2120589, 2382648–2382649, 2442574–2524367 for **1–2**, **4–8**, **10**, **12–15**, **17–29**, **19HCl**, **21HCl** and **23HCl**. Copies of this information may be obtained free of charge from The Director, CCDC, 12 Union Road, Cambridge CB2 1EY, UK (fax: +44-1223-336033; e-mail: deposit@ccdc.cam.ac.uk or www: http://www.ccdc.cam.ac.uk).

DFT calculations

All calculations were performed using the Gaussian 16 program.⁶¹ Reaction energy profiles were computed at the B3LYP/cc-pVTZ^{45,46} level of theory, incorporating solvation effects through the polarizable continuum model (PCM)⁴⁴ for toluene. Additionally, dispersion corrections were applied using the D3 version of Grimme's dispersion method.⁶² Frequency analysis at the same level of theory confirmed that all computed structures correspond to minima on the potential energy surface, with transition states exhibiting a single imaginary frequency.

ASSOCIATED CONTENT

Supporting Information

The Supporting Information is available free of charge on the ACS Publications website.

Synthetic procedures, explanation of structures and tautomerism, cif files (PDF)

Complete NMR spectra (DOI: 10.6084/m9.figshare.28816364) of all prepared compounds (PDF), FIDs

Cartesian coordinates for atoms in presented in theoretical part.

AUTHOR INFORMATION

Corresponding Author

* Tomáš Chlupatý: tomas.chlupaty@upce.cz; Aleš Růžička: – ales.ruzicka@upce.cz

Author Contributions

The manuscript was written through contributions of all authors. All authors have given approval to the final version of the manuscript. L.V.: synthesis, investigation, writing; K.P.: characterization, analysis; M.A.S.: DFT; Z.R.: X-ray diffraction analysis; T.C.: investigation, writing, NMR spectroscopy, conceptualization; A.R.: conceptualization, supervision, X-ray diffraction analysis, writing.

ACKNOWLEDGMENT

This work was supported by the Czech Science Foundation Grant No. 25-17434S. This work has been funded by a grant from the Programme Johannes Amos Comenius under the Ministry of Education, Youth and Sports of the Czech Republic [No. CZ.02.01.01/00/23_021/0008593].

M.Sc. Natalia Gira and M.Sc. Emilie Riemlová are thanked for their support with specific synthetic tasks.

REFERENCES

1. Superbases for Organic Synthesis: Guanidines, Amidines, Phosphazenes and Related Organocatalysts, Ishikawa, T., Wiley, Chippinham, 2009. DOI:10.1002/9780470740859
2. Raczyńska, E. D.; Gal, J. F.; Maria, P. C. Enhanced Basicity of Push-Pull Nitrogen Bases in the Gas Phase. *Chem. Rev.* **2016**, *116* (22), 13454–13511. DOI: 10.1021/acs.chemrev.6b00224
3. Taylor, J. E.; Bull, S. D.; Williams, J. M. Amidines, isothioureas, and guanidines as nucleophilic catalysts. *Chem. Soc. Rev.* **2012**, *41* (6), 2109–2121. DOI: 10.1039/C2CS15288F
4. Smedley, C. J.; Homer, J. A.; Gialelis, T. L.; Barrow, A. S.; Koelln, R. A.; Moses, J. E. Accelerated SuFEx Click Chemistry For Modular Synthesis. *Angew. Chem., Int. Ed.* **2022**, *61* (4), e202112375. DOI: 10.1002/anie.202112375
5. Muzyka, C.; Renson, S.; Grignard, B.; Detrembleur, C.; Monbaliu, J. M. Intensified Continuous Flow Process for the Scalable Production of Bio-Based Glycerol Carbonate. *Angew. Chem., Int. Ed.* **2024**, *63* (10), e202319060. DOI: 10.1002/anie.202319060
6. Mannisto, J. K.; Sahari, A.; Lagerblom, K.; Niemi, T.; Nieger, M.; Sztano, G.; Repo, T. One-Step Synthesis of 3,4-Disubstituted 2-Oxazolidinones by Base-Catalyzed CO₂ Fixation and Aza-Michael Addition. *Chem. Eur. J.* **2019**, *25* (44), 10284–10289. DOI: 10.1002/chem.201902451
7. Mannisto, J. K.; Pavlovic, L.; Heikkinen, J.; Tiainen, T.; Sahari, A.; Maier, N. M.; Rissanen, K.; Nieger, M.; Hopmann, K. H.; Repo, T. N-Heteroaryl Carbamates from Carbon Dioxide via Chemoselective Superbase Catalysis: Substrate Scope and Mechanistic Investigation. *ACS Catal.* **2023**, *13* (17), 11509–11521. DOI: 10.1021/acscatal.3c02362
8. Morack, T.; Myers, T. E.; Karas, L. J.; Hardy, M. A.; Mercado, B. Q.; Sigman, M. S.; Miller, S. J. An Asymmetric Aromatic Finkelstein Reaction: A Platform for Remote Diarylmethane Desymmetrization. *J. Am. Chem. Soc.* **2023**, *145* (41), 22322–22328. DOI: 10.1021/jacs.3c08727
9. Chinn, A. J.; Kim, B.; Kwon, Y.; Miller, S. J. Enantioselective Intermolecular C–O Bond Formation in the Desymmetrization of Diarylmethines Employing a Guanidinylated Peptide-Based Catalyst. *J. Am. Chem. Soc.* **2017**, *139* (49), 18107–18114. DOI: 10.1021/jacs.7b11197
10. Barton, D.; Elliott, J.; Géro, S. Synthesis and properties of a series of sterically hindered guanidine bases. *J. Chem. Soc., Perkin Trans. 1*, **1982**, 2085–2090. DOI: 10.1039/P19820002085.
11. Berlinck, R. G. S.; Bertonha, A. F.; Takaki, M.; Rodriguez, J. P. G. The chemistry and biology of guanidine natural products. *Nat. Prod. Rep.* **2017**, *34* (11), 1264–1301. DOI: 10.1039/C7NP00037E
12. Somberg, N. H.; Sučec, I.; Medeiros-Silva, J.; Jo, H.; Beres, R.; Syed, A. M.; Doudna, J. A.; Hong, M. Oligomeric State and Drug Binding of the SARS-CoV-2 Envelope Protein Are Sensitive to the Ectodomain. *J. Am. Chem. Soc.* **2024**, *146* (35), 24537–24552. DOI: 10.1021/jacs.4c07686
13. von Itzstein, M. The war against influenza: discovery and development of sialidase inhibitors. *Nat. Rev. Drug Discovery*, **2007**, *6*, 967–974. DOI: 10.1038/nrd2400.
14. Gund, P. Guanidine, trimethylenemethane, and "Y-delocalization." Can acyclic compounds have "aromatic" stability? *J. Chem. Educ.* **1972**, *49*, 100–103. DOI: 10.1021/ed049p100.
15. Pei, T.; Zhou, L.; Zhang, Q.; Ma, D.; Bai, Y.; Yin, Q.; Xie, C. Studies on structure, NLO properties of a new organic NLO crystal: guanidinium 3,5-dihydroxybenzoate. *J. Mater. Sci: Mater. Electron.* **2019**, *30*, 2994–3003. DOI: 10.1007/s10854-018-00578-1
16. Sengupta, D.; Gómez-Torres, A.; Fortier, S. *Guanidinate, Amidinate, and Formamidinate Ligands*. Editor(s): Edwin C. Constable, Gerard Parkin, Lawrence Que Jr, *Comprehensive Coordination Chemistry III*, Elsevier, 2021, Pages 366-405, ISBN 9780081026892, DOI: 10.1016/B978-0-08-102688-5.00070-2
17. Bailey, P. J.; Pace, S. The coordination chemistry of guanidines and guanidates. *Coord. Chem. Rev.* **2001**, *214* (1), 91–141. DOI: 10.1016/S0010-8545(00)00389-1
18. Coles, M. P. Application of neutral amidines and guanidines in coordination chemistry. *Dalton Trans.* **2006**, (8), 985–1001. DOI: 10.1039/B515490A
19. Jones, C. Bulky guanidates for the stabilization of low oxidation state metallacycles. *Coord. Chem. Rev.* **2010**, *254* (11-12), 1273–1289. DOI: 10.1016/j.ccr.2009.07.014
20. Carrillo-Hermosilla, F.; Fernández-Galán, R.; Ramos, A.; Elorriaga, D. Guanidates as Alternative Ligands for Organometallic Complexes. *Molecules* **2022**, *27* (18), 5962–5992. DOI: 10.3390/molecules27185962.
21. Alonso-Moreno, C.; Antinolo, A.; Carrillo-Hermosilla, F.; Otero, A. Guanidines: from classical approaches to efficient catalytic syntheses. *Chem. Soc. Rev.* **2014**, *43* (10), 3406–3425. DOI: 10.1039/C4CS00013G
22. Takeuchi, K.; Nakayama, A.; Tanino, K.; Namba, K. Facile Guanidine Formation under Mild Acidic Conditions. *Synlett* **2016**, *27* (18), 2591–2596. DOI: 10.1055/s-0035-1562478
23. Maierhaba, J.; Bulunuer, Y.; Abudurehman, W. Catalyst and Additive-Free Direct Synthesis of N-Sulfonyl Guanidines. *Chinese J. Org. Chem.* **2024**, *44* (4), 1276–1283. DOI: 10.6023/cjoc202308019
24. Zhang, W.-X.; Xu, L.; Xi, Z. Recent development of synthetic preparation methods for guanidines via transition metal catalysis. *Chem. Commun.* **2015**, *51* (2), 254–265. DOI: 10.1039/C4CC05291A
25. Levallet, C.; Lerpiniere, J.; Ko, S.Y. The HgCl₂-promoted guanidination reaction: The scope and limitations. *Tetrahedron* **1997**, *53* (14), 5291–5304. DOI: 10.1016/S0040-4020(97)00193-2

26. Tsubokura, K.; Iwata, T.; Taichi, M.; Kurbangalieva, A.; Fukase, K.; Nakao, Y.; Tanaka, K. Direct Guanylation of Amino Groups by Cyanamide in Water: Catalytic Generation and Activation of Unsubstituted Carbodiimide by Scandium(III) Triflate. *Synlett* **2014**, *25* (9), 1302–1306. DOI: 10.1055/s-0033-1341080
27. Xu, L.; Wang, Z.; Zhang, W.-X.; Xi, Z. Rare-Earth Metal Tris(trimethylsilylmethyl) Anionic Complexes Bearing One 1-Phenyl-2,3,4,5-tetrapropylcyclopentadienyl Ligand: Synthesis, Structural Characterization, and Application. *Inorg. Chem.* **2012**, *51* (21), 11941–11948. DOI: 10.1021/ic3018369
28. Banerjee, I.; Sagar, S.; Lorber, C.; Panda, T. K. Catalytic addition reactions of amines, thiols, and diphenyl-phosphine oxides to heterocumulenes using a bridging Sulfonylimido titanium(IV) complex. *Z. Anorg. Allgem. Chem.* **2022**, *648* (18), e202200188. DOI: 10.1002/zaac.202200188
29. Gao, Y.; Carta, V.; Pink, M.; Smith, J. M. Catalytic Carbodiimide Guanylation by a Nucleophilic, High Spin Iron(II) Imido Complex. *J. Am. Chem. Soc.* **2021**, *143* (14), 5324–5329. DOI: 10.1021/jacs.1c02068
30. Pottabathula, S.; Royo, B. First iron-catalyzed guanylation of amines: a simple and highly efficient protocol to guanidines. *Tetrahedron Lett.* **2012**, *53* (38), 5156–5158. DOI: 10.1016/j.tetlet.2012.07.065
31. Kantam, M. L.; Priyadarshini, S.; Joseph, P. J. A.; Srinivas, P.; Vinu, A.; Klabunde, K. J.; Nishina, Y. Catalytic guanylation of aliphatic, aromatic, heterocyclic primary and secondary amines using nanocrystalline zinc(II) oxide. *Tetrahedron* **2012**, *68* (29), 5730–5737. DOI: 10.1016/j.tet.2012.05.044
32. Muthuvinothini, A.; Stella, S. L-Cysteine capped Zn nanoparticles catalyzed synthesis of guanidines. *Synth. Commun.*, **2021**, *51*, 461–470. DOI: 10.1080/00397911.2020.1837169.
33. Ong, T.-G.; O'Brien, J. S.; Korobkov, I.; Richeson, D. S. Facile and Atom-Efficient Amidolithium-Catalyzed C–C and C–N Formation for the Construction of Substituted Guanidines and Propiolamidines. *Organometallics* **2006**, *25* (20), 4728–4730. DOI: 10.1021/om060539r
34. Lachs, J. R.; Barrett, A. G. M.; Crimmin, M. R.; Kociok-Köhn, G.; Hill, M. S.; Mahon, M. F.; Procopiou, P. A. Heavier Group-2-Element Catalyzed Hydroamination of Carbodiimides. *Eur. J. Inorg. Chem.*, **2008**, *26*, 4173–4179. DOI: 10.1002/ejic.200800613
35. Karmakar H.; Anga S.; Panda T. K.; Chandrasekhar V. Aluminium alkyl complexes supported by imino-phosphoramidate ligand as precursors for catalytic guanylation reactions of carbodiimides. *RSC Adv.*, **2022**, *12* (8), 4501–4509. DOI: 10.1039/D2RA00242F
36. Nayak, D. K.; Sarkar, N.; Sampath, C. M.; Sahoo, R. K.; Nembenna, S. Organoaluminum Catalyzed Guanylation and Hydroboration Reactions of Carbodiimides. *Z. Anorg. Allgem. Chem.* **2022**, *648* (19), e202200116. DOI: 10.1002/zaac.202200116
37. Du, Z.; Wen, X.; Pang, Z. Hydroamination of Carbodiimides Catalyzed by Lithium Triethylborohydride. *Synthesis*, **2023**, *55*, 1079–1088. DOI: 10.1055/a-1979-8930.
38. Antiñolo, A.; Carrillo-Hermosilla, F.; Fernández-Galán, R.; Martínez-Ferrer, J.; Alonso-Moreno, C.; Bravo, I.; Moreno-Blázquez, S.; Salgado, M.; Villaseñor, E.; Albaladejo, J. Tris(pentafluorophenyl)borane as an efficient catalyst in the guanylation reaction of amines. *Dalton Trans.* **2016**, *45* (26), 10717–10729. DOI: 10.1039/C6DT01237J.
39. Porashar, B.; Choudhury, C.; Saikia, A. K. Synthesis of 2,4-Diaminoquinazolines and 2-Amino-4-iminoquinazolines via Substrate-Controlled Annulation of 2-Aminobenzonitriles and Carbodiimides. *Chemistry Select*, **2025**, *10*, e202405899. DOI: 10.1002/slct.202405899.
40. Aho, J. A. S.; Mannisto, J. K.; Mattila, S. P. M.; Hallamaa, M.; Deska J. Guanidium Unmasked: Repurposing Common Amide Coupling Reagents for the Synthesis of Pentasubstituted Guanidine Bases *J. Org. Chem.* **2025**, *90* (7), 2636–2643 DOI: 10.1021/acs.joc.4c02645.
41. Ong, T. G.; Yap, G. P. A.; Richeson, D. S. Catalytic Construction and Reconstruction of Guanidines: Ti-Mediated Guanylation of Amines and Transamination of Guanidines. *J. Am. Chem. Soc.*, **2003**, *125*, 8100–8101. DOI: 10.1021/ja035716j.
42. Zhang, W.-X.; Nishiura, M.; Hou, Z. Catalytic Addition of Amine N-H Bonds to Carbodiimides by Half-Sandwich Rare-Earth Metal Complexes: Efficient Synthesis of Substituted Guanidines through Amine Protonolysis of Rare-Earth Metal Guanidates. *Chem. Eur. J.* **2007**, *13*, 4037–4051. DOI: 10.1002/chem.200601383.
43. Zhang, W.-X.; Li, D.; Wang, Z.; Xi, Z. Alkyl Aluminum-Catalyzed Addition of Amines to Carbodiimides: A Highly Efficient Route to Substituted Guanidines. *Organometallics*, **2009**, *28*, 882–887. DOI: 10.1021/om801035t.Becke, A. D. Density-functional thermochemistry. III. The role of exact exchange. *J. Chem. Phys.* **1993**, *98* (7), 5648–5652. DOI: 10.1063/1.464913
44. Tomasi, J.; Mennucci, B.; Cammi, R. Quantum Mechanical Continuum Solvation Models. *Chem. Rev.* **2005**, *105*, 2999–3094. <https://doi.org/10.1021/cr9904009>
45. Becke, A. D. Density-functional thermochemistry. III. The role of exact exchange. *J. Chem. Phys.* **1993**, *98* (7), 5648–5652. DOI: 10.1063/1.464913
46. Dunning, T. H. Gaussian basis sets for use in correlated molecular calculations. I. The atoms boron through neon and hydrogen. *J. Chem. Phys.* **1989**, *90* (2), 1007–1023. DOI: 10.1063/1.456153
47. Dorokhov, V. A.; Shagova, É. A.; Novikova, T. S.; Sheremetev, A. B.; Khmel'nitskii, L. I. Synthesis of guanidinofurazans from aminofurazans and carbodiimides. *Russ. Chem. Bull.* **1988**, *37*, 2128–2131. DOI: 10.1007/bf00953419
48. Kurzer, F.; Sanderson P. M. 38. Heterocyclic compounds from urea derivatives. Part V. Synthesis and cyclisation of N-o-hydroxyphenyl-N''-diarylguanidines. *J. Chem. Soc.* **1963**, 240–245, DOI: 10.1039/JR9630000240
49. Kurzer, F.; Sanderson P. M. 43. Heterocyclic compounds from urea derivatives. Part III. Synthesis and cyclisation of isothiureas derived from o-aminothiophenol and diarylcarbodi-imides. *J. Chem. Soc.* **1962**, 230–236, DOI: 10.1039/JR9620000230

50. Snedker, S. J. C. The mechanism of the formation of triphenylguanidine and phenylthiocarbimide from thiocarbanilide. *Transactions. J. Chem. Technol. Biotechnol.* **1926**, *45* (41), T343-T354. DOI: 10.1002/jctb.5000454111
51. Weith, W. Ueber Carbodiphenylimid. *Ber. Dtsch. Chem. Ges.* **1874**, *7* (1), 10–16. DOI: 10.1002/cber.18740070105
52. Weith, W. Ueber Tetrphenylguanidin und Diphenylcyanamid. *Ber. Dtsch. Chem. Ges.* **1874**, *7* (1), 843–853. DOI: 10.1002/cber.187400701271
53. Huhn, A. Beiträge zur Kenntniss der aromatischen Carbodiimide. *Ber. Dtsch. Chem. Ges.*, **1886** *19* (2), 2404–2414. DOI: 10.1002/cber.188601902170
54. Busch, M.; Blume, G.; Plungs, E. Zur Kenntnis der Carbodiimide. *J. Prakt. Chem.* **1909**, *79* (1), 513–546. DOI: 10.1002/prac.19090790136
55. Patt, S. L.; Shoolery, J. N. Attached proton test for carbon-13 NMR. *J. Magn. Reson.* **1982**, *46*, 535–539. DOI: 10.1016/0022-2364(82)90105-6
56. Otwinowski, Z.; Minor, W. Processing of X-ray diffraction data collected in oscillation mode. *Methods Enzymol* **1997**, *276*, 307–326. DOI: 10.1016/S0076-6879(97)76066-X
57. P. Coppens In: F.R. Ahmed, S.R. Hall, C.P. Huber Editors, *Crystallographic Computing*, **1970**, pp. 255 – 270, Copenhagen, Munksgaard.
58. Altomare, A.; Cascarano, G.; Giacovazzo, C.; Guagliardi, A. Early finding of preferred orientation: a new method. *J. Appl. Cryst.* **1994**, *27*, 1045–1050. DOI: 10.1107/S002188989400422X.
59. Sheldrick, G. M. SHELXL-97, University of Göttingen: Göttingen, **2008**.
60. Sheldrick, G. M. Crystal structure refinement with SHELXL. *Acta Cryst. C* **2015**, *71*, 3–8. DOI: 10.1107/S2053229614024218.
61. Gaussian 16, Revision C.01, Frisch, M. J.; Trucks, G. W.; Schlegel, H. B.; Scuseria, G. E.; Robb, M. A.; Cheeseman, J. R.; Scalmani, G.; Barone, V.; Petersson, G. A.; Nakatsuji, H.; Li, X.; Caricato, M.; Marenich, A. V.; Bloino, J.; Janesko, B. G.; Gomperts, R.; Mennucci, B.; Hratchian, H. P.; Ortiz, J. V.; Izmaylov, A. F.; Sonnenberg, J. L.; Williams-Young, D.; Ding, F.; Lipparini, F.; Egidi, F.; Goings, J.; Peng, B.; Petrone, A.; Henderson, T.; Ranasinghe, D.; Zakrzewski, V. G.; Gao, J.; Rega, N.; Zheng, G.; Liang, W.; Hada, M.; Ehara, M.; Toyota, K.; Fukuda, R.; Hasegawa, J.; Ishida, M.; Nakajima, T.; Honda, Y.; Kitao, O.; Nakai, H.; Vreven, T.; Throssell, K.; Montgomery, J. A., Jr.; Peralta, J. E.; Ogliaro, F.; Bearpark, M. J.; Heyd, J. J.; Brothers, E. N.; Kudin, K. N.; Staroverov, V. N.; Keith, T. A.; Kobayashi, R.; Normand, J.; Raghavachari, K.; Rendell, A. P.; Burant, J. C.; Iyengar, S. S.; Tomasi, J.; Cossi, M.; Millam, J. M.; Klene, M.; Adamo, C.; Cammi, R.; Ochterski, J. W.; Martin, R. L.; Morokuma, K.; Farkas, O.; Foresman, J. B.; Fox, D. J. Gaussian, Inc., Wallingford CT, **2016**.
62. Grimme, S.; Antony, J.; Ehrlich, S.; Krieg, H. A consistent and accurate ab initio parametrization of density functional dispersion correction (DFT-D) for the 94 elements
- H-Pu. *J. Chem. Phys.* **2010**, *132*, 154104. DOI: 10.1063/1.3382344